

## IV–VI Nanocrystal–polymer solar cells

Karolina P. Fritz<sup>a</sup>, Serap Guenes<sup>b,1</sup>, Joseph Luther<sup>c</sup>,  
Sandeep Kumar<sup>a</sup>, N. Serdar Sariciftci<sup>b,\*</sup>, Gregory D. Scholes<sup>a,\*\*</sup>

<sup>a</sup> Department of Chemistry and Institute for Optical Sciences, University of Toronto, 80 St. George Street,  
Toronto, Ont. M5S 3H6, Canada

<sup>b</sup> Linz Institute for Organic Solar Cells (LIOS), Johannes Kepler University, Altenbergerstr. 69, 4040 Linz, Austria

<sup>c</sup> National Renewable Energy Laboratory, 1617 Cole Boulevard, Golden, CO 80401, USA

Received 28 May 2007; received in revised form 17 August 2007; accepted 3 September 2007

Available online 7 September 2007

### Abstract

Processes are investigated for the fabrication of hybrid bilayer photovoltaic (PV) devices consisting of IV–VI nanocrystals (NCs) having near-infrared optical gaps and an organic conductive polymer. Our design utilizes PbS NCs spin-cast onto an indium tin oxide (ITO) coated glass slide, covered with a poly(3-hexylthiophene-2,5-diyl) (P3HT) layer. We demonstrate here that the removal of the surface ligand, by pre-rinsing the NCs and subsequent annealing, generates a smoother film with a greater degree of cross-linking between the NCs. Additionally, a post-production treatment enhances the interfacial layer and improves charge carrier separation and mobility, rendering better performing solar cells. Further, results using PbSe NCs indicate the method can be adapted to similar systems. The method proposed here was designed to optimize more independently the polymer and nanocrystal components of the device and, to an extent, the interface between them.

© 2007 Elsevier B.V. All rights reserved.

**Keywords:** Nanocrystals; PbS; Solar cells; Photovoltaic devices; Near-infrared

### 1. Introduction

Solar cells based on conjugated polymer active layers have attracted considerable attention in recent years as a way of decreasing the cost of photovoltaic energy conversion [1]. While the low cost and ease of processing is driving further research in this type of organic solar cell, the underlying science has generated much interest across a range of disciplines [2]. Successful devices are typically based on the use of bulk heterojunctions or hybrid blends [1,3–12] which provide a large contact area between the donor and acceptor species. The combination of many factors determine the energy conversion efficiency of solar cells [13,14], however, it is clear that the incident spectrum captured by a device is controlled, and limited by, the absorption of the active layer. Recent work has explored possibilities

for expanding the cross-section of absorbed light by designing near-infrared (NIR) absorbing polymers [15–17], incorporating NIR-absorbing semiconductor nanocrystals (NCs) into hybrid devices [18–20], or adding an intrinsic “antenna” layer [21,22].

Effective harvesting of sunlight for solar energy conversion ideally captures part of the near-infrared spectral region. One way to achieve that is through the use of nanostructured PbS or PbSe materials, which have absorption edges that can be size-tuned through the near-infrared [23]. Furthermore, the prediction [24] and subsequent experimental evidence [25–27] for multiple exciton generation (carrier multiplication), whereby the absorption of one photon results in the formation of more than one electron–hole pair, further motivates the fabrication of lead chalcogenide-based solar cells. For example, it is important to discover whether multiple exciton generation can increase the energy conversion efficiency of a device—that is, can the multi-exciton states be harvested to provide free carriers?

Despite the fact that PbS and PbSe appear to possess the required fundamental properties to be used in a high performance hybrid NC/conjugated polymeric solar cell, studies to date of PbS/MEH-PPV [18] (poly[2-methoxy-5-(2-ethylhexyloxy-*p*-phenylenevinylene)]) or PbSe/P3HT [19]

\* Corresponding author.

\*\* Corresponding author. Tel.: +1 416 946 7532; fax: +1 416 978 8775.

E-mail addresses: [serdar.sariciftci@jku.at](mailto:serdar.sariciftci@jku.at) (N.S. Sariciftci),  
[gscholes@chem.utoronto.ca](mailto:gscholes@chem.utoronto.ca) (G.D. Scholes).

<sup>1</sup> Current address: Department of Physics, Yildiz Technical University, Davutpasa Campus, 34220 Davutpasa, Esenler, Istanbul, Turkey.

(poly(3-hexylthiophene-2,5-diyl)) devices report very low energy conversion efficiencies; orders of magnitude lower than comparable CdSe or CdTe/conjugated polymer devices [13,28]. It is important now to identify bottlenecks that limit the operation of these devices and to elucidate a means to improve the design and processing of NIR IV–VI nanocrystal-based solar cells. Here we report a layered device architecture and processing procedure to improve the energy conversion efficiency significantly. We systematically investigate the role played by quantum size effects and spectral coverage, and further compare the incorporation of PbS and PbSe NCs into the active layer. On that basis, we discuss future directions for design of these devices.

An important consideration in processing NC-polymer hybrid solar cells is the passivating layer of organic ligands adsorbed to the NC surface. These organic ligands stabilize the size and shape of the NCs, prevent aggregation and growth to bulk, and furthermore determine the NC solubility. However, these organic ligands also act as barriers for the flow of charge carriers in and out of the NCs. Overall the organic ligands therefore inhibit carrier mobility in PV devices, and their bulkiness and/or the thermodynamics of chain conformation and mixing, often can cause phase separation. On the other hand, a poorly passivated NC surface can lead to carrier recombination through a large density of surface trap states. As a compromise, small ligands like pyridine are typically exchanged onto CdSe NCs natively capped with TOPO [29,30]. Similarly, it was shown that for PbS NCs prepared with oleate ligands, a post-synthesis ligand exchange to short-chain amines helped to increase the external and internal electroluminescence (EL) quantum efficiency of PbS NCs [31,32].

Since the post-synthesis ligand exchange treatment on PbS NCs was established there have been a few NIR NC-based PV devices reported. First, Zhang et al. [33] demonstrated that a bulk heterojunction hybrid solar cell with a blend of MEH-PPV and PbS NCs ( $\lambda_{\text{abs}} = 935$  and 1300 nm) coated with short-chain amines were more efficient than PbS NCs coated with the original oleate ligands. This was attributed to the charge carriers being able to tunnel through the ligand barrier, or to transfer directly from the conjugated polymer to NC surface sites left free by incomplete ligand exchange process. However reported efficiencies were low due to the poor short-circuit current ( $I_{\text{sc}}$ ) of 250 nA and an open-circuit voltage ( $V_{\text{oc}}$ ) of 0.47 V. McDonald et al. [18] later reported characterization of a bulk heterojunction hybrid solar cell where PbS NCs ( $\lambda_{\text{abs}} = 1200$  nm) with ligand-exchanged amines were incorporated into a MEH-PPV matrix to achieve a maximum internal quantum efficiency of  $\sim 0.006\%$ .

In another study, Maria et al. [34] demonstrated a bilayer PV device of PbS NCs ( $\lambda_{\text{abs}} = 1260$  nm) with ligand-exchanged short-chain amines and poly-3(octylthiophene) (P3OT) polymer that had an internal quantum efficiency of 11.3% and an external quantum efficiency exceeding 1% for an infrared PV response at  $\lambda = 720$  nm. However, no overall energy conversion efficiency for the device was mentioned. Cui et al. [35] recently reported a bulk heterojunction solar cell that contained PbSe NCs ( $\lambda_{\text{abs}} = 1500$  nm) coated with oleate ligands in a P3HT matrix. The device exhibited an incident monochromatic photon to current conversion efficiency (IPCE) of 1.3% at  $\lambda = 805$  nm, and an

overall power conversion efficiency of 0.14% was achieved. In conclusion, most of the NIR NCs PV devices reported recently have been of bulk heterojunction type and/or have substituted short-chain amines for the oleate ligands. Besides such architectures, another possible configuration for a photovoltaic device is a bilayer device consisting of a layer by layer coating of NCs and polymer. In this report we investigate the optimization of the power conversion efficiency of a bilayer device using a ligand and removal process, rather than a ligand exchange, to assist photo-induced charge transfer and carrier mobility. We examine devices fabricated using different sizes of PbS and PbSe NCs. The new method proposed here was designed to optimize independently the polymer and nanocrystal components of the device and, to an extent, their interface.

## 2. Experimental

### 2.1. Synthesis of PbX nanocrystals

All chemicals were purchased from Sigma–Aldrich. PbS NCs were synthesized as previously reported [23]. In general, a typical synthesis was carried out in a 3-neck-flask. The lead oleate precursor was prepared by heating PbO in oleic acid (OA) at concentrations from 0.1 to 0.5 M under argon at 150 °C. Then bis(trimethylsilyl)sulfide (TMS) in 1-octadecene (ODE) was rapidly injected into the flask. In order to produce different sizes of PbS NCs the TMS in ODE was injected at temperatures ranging from 50 to 150 °C. Also, different initial molar ratios of Pb:S:OA were used. After growth the PbS NCs were isolated with ethyl acetate then redispersed in chloroform.

PbSe NCs were synthesized as previously reported [36]. Typically, the synthesis was carried out in a 3-neck-flask and under argon. A mixture of 2.5 g of PbO, 7.5 g of OA, and 18.5 g of ODE were heated to 150 °C. Then the temperature was raised to 180 °C and 1.5 g of Se powder in 20 mL of tri-octyl phosphine (TOP) was injected. The flask was quickly removed from the heat and cooled down to 80 °C using a cold water bath. Next 25 mL of hexane was added until the temperature dropped to 30 °C. The resulting PbSe NCs were isolated with acetone, and redispersed in chloroform.

### 2.2. Device preparation

A 1.5 cm  $\times$  1.5 cm indium tin oxide (ITO) coated glass substrate (Merck KG Darmstadt) with an ITO thickness of  $\sim 120$  nm and a surface resistance  $< 15 \Omega/\text{cm}^2$  was used. The ITO was patterned by etching it with an acid mixture of  $\text{HCl}_{\text{conc}}:\text{HNO}_{\text{conc}}:\text{H}_2\text{O}$  (4.6:0.4:5) for  $\sim 30$  min. The substrates were then cleaned with an ultrasonic bath of acetone first, followed by *iso*-propanol, and finally dried with an  $\text{N}_2$  flow.

About 45 mg/mL of PbS or 100 mg/mL of PbSe NCs were diluted with ethyl acetate (EtAc) and chloroform with volume ratios of 1:6 (EtAc: $\text{CHCl}_3$ ). This mixture was spin-cast at 8000 rpm and annealed gradually to 200 °C in a vacuum oven. A 1 wt% of regioregular poly(3-hexylthiophene-2,5-diyl) (Rieke Metals Inc.) in chloroform was prepared and drop cast onto the PbS films. Then 160 nm of gold was thermally evaporated onto

the film in a vacuum better than  $10^{-5}$  mbar. After fabrication the electrical properties of the devices were measured before and after they were further annealed to  $100^\circ\text{C}$  for 1 h on a hot plate.

### 2.3. Device characterization

An inert argon environment inside a glove box system (MB 200 from MBraun) was used for the electrical characterizations. The current versus voltage curves were measured with a Keithley 236 source measure unit under an illumination intensity of  $100\text{ mW/cm}^2$  with a solar simulator source (K.H. Steuernagel Lichttechnik GmbH) simulating AM 1.5 conditions. The devices were illuminated through the ITO coated glass. Under ambient conditions the surface morphology measurements were carried out with a Digital Instruments Dimension 3100 atomic force microscope (AFM) in tapping mode.

In order to measure the incident photon to collected electron efficiency (IPCE) response of the device, the samples were illuminated under ambient conditions with light from a halogen lamp passing a monochromator (band width  $< 5\text{ nm}$ ) and through a mechanical chopper. A Stanford Research Systems Model SR810 DSP lock-in amplifier was used to relate the photocurrent of the solar cell to the photon flux, which was calibrated with a silicon reference diode up to  $1100\text{ nm}$ . The external quantum efficiency or the IPCE was calculated using the following formula that has been explained in Ref. [37]:

$$\text{IPCE}(\%) = \frac{1240 I_{\text{sc}}}{(\lambda P_{\text{in}})} \quad (1)$$

where  $I_{\text{sc}}$  is the short circuit current density ( $\mu\text{A/cm}^2$ ),  $\lambda$  the incident photon wavelength (nm), and  $P_{\text{in}}$  is the monochromatic light incidence ( $\text{W/m}^2$ ).

## 3. Results and discussion

The effectiveness of hybrid solar cells depends, among other effects, on the efficacy of photocurrent generation at the nanocrystal/polymer interface. In general, bulk heterojunction solar cells consist of an interpenetrating network of donor and acceptor components for efficient charge separation [38]. It is therefore important that the donor and the acceptor mix homogeneously over a length scale of their exciton diffusion length (approx.  $10\text{--}20\text{ nm}$  in polymers). In hybrid solar cells the organic ligands adsorbed to the surface of the NCs are the key, and yet limiting, factor. For example, in our early trials to make bulk heterojunction hybrid solar cells we attempted to mix PbS NCs coated with oleate or with ligand exchanged short-chain amines with P3HT. The organic ligands inhibited mixing of the PbS NCs with the P3HT matrix. The films prepared from these solutions always contained agglomerations of PbS NCs and P3HT domains, and the coarse phase separation of these components rendered the solar cells less efficient.

To remedy this situation, we attempted a new method for removal of organic ligands from the surface of the QDs and further designing a bilayer device as depicted in Fig. 1, where

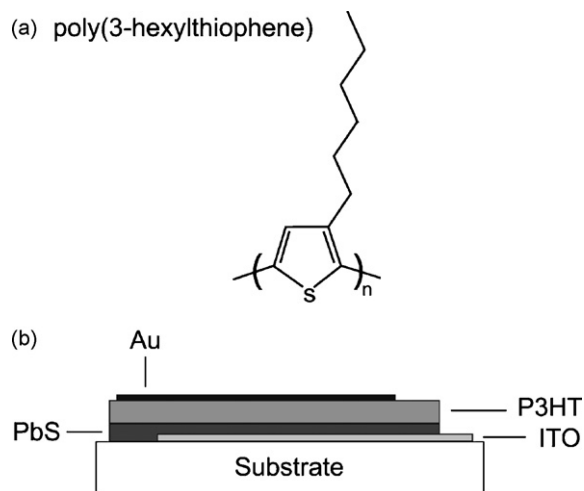


Fig. 1. (a) Regioregular poly(3-hexylthiophene-2,5-diyl). (b) Schematic of the structure of the bilayer hybrid solar cell.

PbS NCs were used as the electron transporting layer and P3HT was used as the hole transporting layer. This design gave us the advantage to pre-treating and optimizing the PbS (or PbSe) NC film before the P3HT film was deposited. To fabricate a bilayer solar cell, the PbS NCs film needed to be treated to render it insoluble in the P3HT/chloroform solution during the spin-coating of the second layer. It was found that the PbS NCs had to be dissolved in a mixture of ethyl acetate and chloroform before spin-casting. If the ethyl acetate is not a component of the mixture then the films will be soluble to the P3HT solution before or after the heat treatment. After annealing the PbS NCs films at  $200^\circ\text{C}$ , they were found to maintain their integrity upon the casting of the P3HT solution.

We further investigated possible nanocrystal size-dependent effects in PbS NCs solar cells. The different sizes of NCs have different band gaps due to the quantum confinement effect. The different sizes will therefore overlap different portions of the solar spectrum. Hence, one would expect that the light harvesting efficiencies will change with the size of the NCs due to their different profiles within the solar spectrum. An optimum energy conversion efficiency may be obtained by tuning the interplay of absorption cross-section with diminished open-circuit voltage as the band gap is reduced [14,39]. It turned out to be difficult to quantify directly quantum confinement effects in practice because additional factors need to be considered, such as the packing capabilities and the quantity of ligands on the NC surface, which depend on NC size.

First, the packing of the NCs affects the morphology of the films prepared. The size of the NCs influences the interstitial spacing between them, despite “size” being blurred by the ligand and corona. Thus larger NCs, with larger interstitial gaps, tend to produce rougher films and exhibit larger agglomerations within the films. These morphological effects were characterized by atomic force microscopy (AFM). Fig. 2 shows the morphology of the PbS NC films of different sizes before and after the heat treatment. The PbS NC films appear to form small agglomerates before annealing, however after annealing, the surface roughness of the PbS NC films is reduced. A smooth film increases

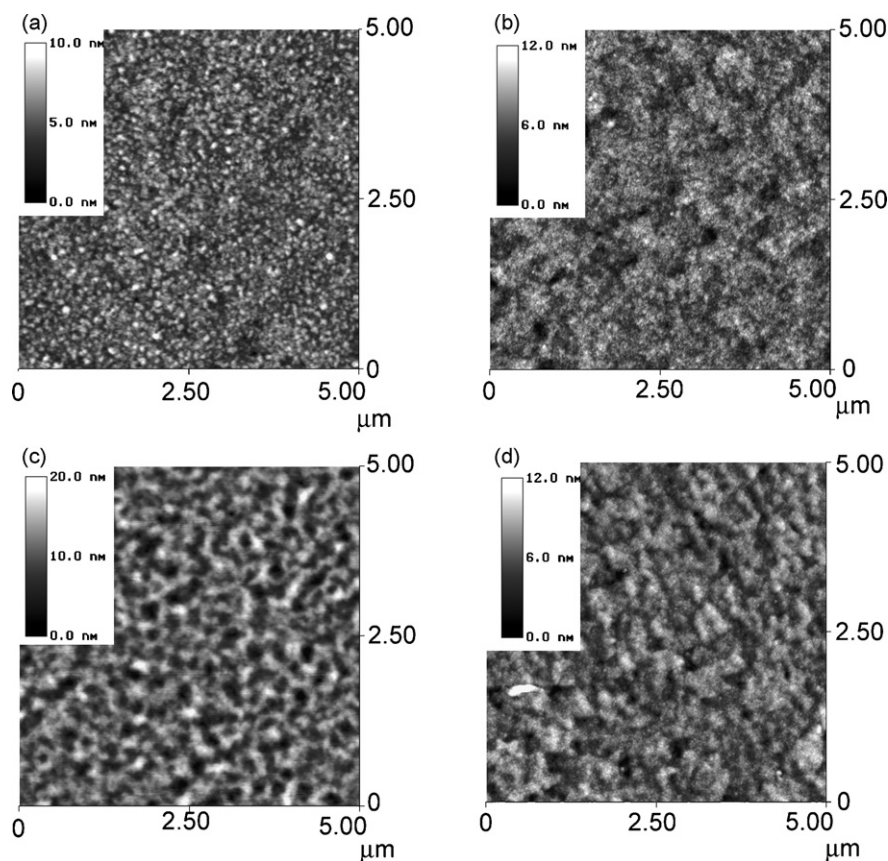


Fig. 2. AFM images of the deposited PbS films taken prior to (left) and after (right) annealing of sample A (a, b) and sample D (c, d). See Table 1 for definition of these samples.

charge carrier transfer and mobility and decreases series resistance, probably as a result of better contacts and thus electronic coupling [40,41].

As discussed in the previous section, the organic ligands adsorbed to the surface of the NCs adversely affect the charge transport. Since larger NCs have high surface area, a lower efficiency will be expected due to less carrier transfers and reduced mobility. On the other hand, a significant quantity of organic ligands could be removed with the addition of ethyl acetate, thereby reducing charge carrier recombination and increasing carrier mobility.

The PV properties of the PbS NCs solar cells were characterized by measuring current–voltage ( $I$ – $V$ ) curves in the dark and

under white light illumination through the ITO side. The characteristic parameters of the PbS NCs solar cells were deduced from the  $I$ – $V$  curves, plotted on linear scales in Fig. 3. The details of the devices are collected in Table 1. From the photocurrent properties collected for different sizes of PbS NCs solar cells no clear size-dependence could be determined.

The spectral response (IPCE) and the absorption spectrum for the different sizes of PbS NCs solar cells are shown in Fig. 4. IPCE data beyond 1100 nm are not reported because the signal was too weak and could not be distinguished from background noise even after calibration correction. The comparison of the spectral response and the optical absorption spectra gives information on the charge carrier generation mechanism.

Table 1  
Measured performance characteristics of devices A–D

Sample	PbS $\lambda_{\text{film}}$ (nm)	Post-production annealing	$I_{\text{SC}}$ (mA/cm <sup>2</sup> )	$V_{\text{OC}}$ (mV)	FF <sup>a</sup>	Efficiency (%)
A	810	Before	0.05	200	0.32	0.0032
		After	0.12	400	0.38	0.0182
B	865	Before	0.06	100	0.39	0.0023
		After	0.13	200	0.29	0.0075
C	1050	Before	0.07	200	0.36	0.0050
		After	0.11	350	0.44	0.0169
D	1145	Before	0.08	300	0.46	0.0110
		After	0.13	400	0.38	0.0198

<sup>a</sup> Fill factor (FF).

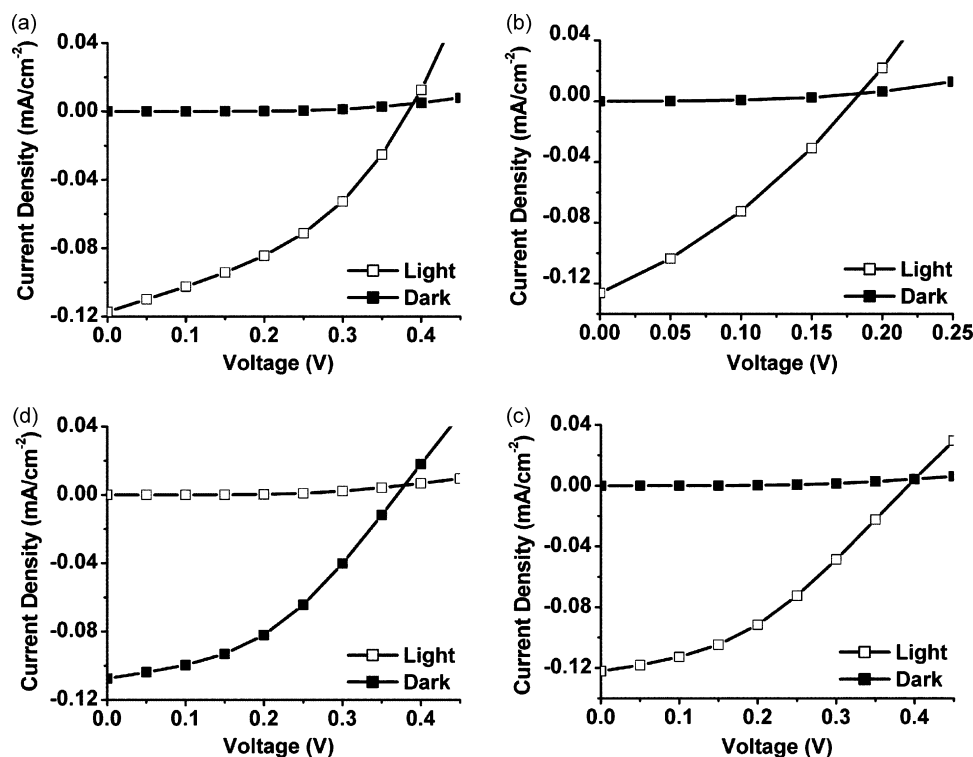


Fig. 3.  $I$ - $V$  characteristics of the PbS NCs samples A–D (a–d) on a linear scale after the post-production heat treatment. See Table 1 for definition of these samples.

As previously reported both PbS NCs and P3HT contribute to the charge carrier generation [42]. P3HT has a broad absorption with an absorption maximum at 550 nm. IPCE data shorter than 700 nm is attributed to the P3HT and are not shown in our figure. The spectral response at wavelengths longer than 700 nm is accredited to the PbS NCs absorption.

The advantage of using the method reported here to prepare solar cells is the use of ethyl acetate in the PbS NCs film treatment. Our results indicate ethyl acetate aids in the partial removal of oleate ligands from the surface of the PbS NCs, leaving free surface sites. In the first step of the procedure, copious quantities of ethyl acetate were used to isolate the PbS NCs from the synthesis residue because ethyl acetate only partially precipitates the PbS NCs. Subsequently, the PbS NCs were redissolved in chloroform and further diluted with a mixture of ethyl acetate and chloroform. The supplementary addition of ethyl acetate further facilitates the removal of more oleate ligands from the PbS NCs surface.

In the next step, the PbS NC solution was spin-cast onto slides and the resulting films were gradually heated to 200 °C in a vacuum oven. This heat treatment eliminates unwanted organics with boiling points lower than 200 °C, such as ethyl acetate and chloroform, resulting in interspatial vacancies. If a temperature greater than 200 °C was used, the films turned from light brown to black indicating PbS bulk. When the films were removed from the oven, they were insoluble to the (chloroform-based) P3HT solution. This insolubility supports the notion that significant amounts of oleate ligands were removed from the surface of the NCs (since solubility properties depend on the adsorbed ligands). Given the partial removal of oleate ligands from the NC surface, and the elimination of the other organic compounds,

the NCs had the opportunity to increase their apposition to one another and to cross-link with adjacent NCs surfaces [43,44]. This proximity has been shown to improve electron transport between the NCs [45,46]; therefore we expect this to improve the efficiency of the bilayer hybrid solar cell.

The post-production annealing of the solar cell increases the mobility of the holes in the polymer. It has been shown that when a polymer, such as P3HT, is thermally annealed slowly above its glass transition temperature an enhancement in crystallinity takes place [47]. This crystalline order helps to increase hole conductivity [48,49]. Our results show an overall improvement in the performance of all solar cells after the post-production heat treatment. We systematically studied the time and temperature of the heat treatment to achieve optimal results. Our solar cells performed best after 1 h at 100 °C: we observed an increase in both  $I_{sc}$  and  $V_{oc}$ . Their enhancement is proposed to be due to an increase in the hole mobility in the polymer layer and the removal of shunts, respectively [50].

Furthermore, we speculate that the post-production heat treatment may have improved the interfacial contact between the two layers [49,51,52]. By increasing polymer crystallinity, the polymer better reticulates with the NC at the interface. The resultant mesh increases the mobility and separation of the charge carriers. The performance of the bilayer design presented here still lags considerably behind bulk heterojunction solar cells based on CdSe [53] and PCBM [10]. This might be due to differences in phase segregation and mixing. On the other hand, an inherent advantage of using PbS is the increased absorption capability in the NIR region of sunlight. Here we presented a methodology to improve the interface between PbS/P3HT by partially removing oleate ligands from the surface of the PbS QDs. We observe that

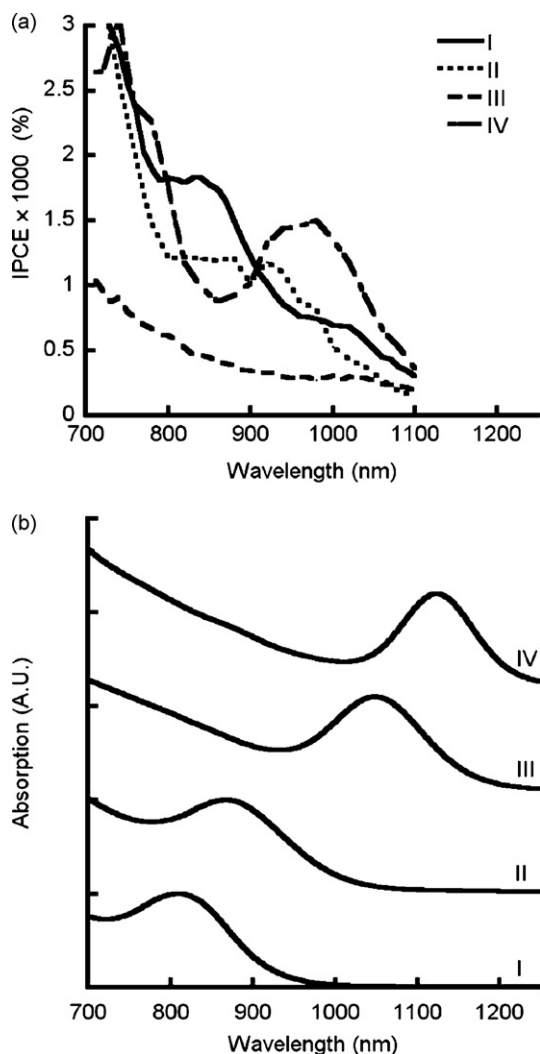


Fig. 4. (a) IPCE spectra of the PbS solar cells. (b) Absorption spectra of the PbS films.

the surface roughness indeed plays an important role in determining the cell performance and can be smoothed by rinsing the PbS layer by a mixture of ethyl acetate and chloroform followed by baking at 200 °C for 1 h.

We have also investigated the incorporation of PbSe NCs into a PV device. PbS and PbSe NCs are IV–VI NIR semiconductors with similar band gaps and syntheses. However, the susceptibility of PbSe NCs to oxidation requires the processing method for each of these PV devices to be uniquely tailored [54]. Therefore, modifications to the procedure described in this report had to be considered. First, the PbSe NCs had to be cleaned with acetone instead of ethyl acetate. If ethyl acetate in combination with methanol was used, then the PbSe NCs agglomerated and turned grayish in color; indicating an increase of size towards bulk, hence eliminating quantum size effects. Next, the spin-coating speed had to be reduced in order to make uniform films due to the initial higher mass used in the preparation of the solution, resulting in rougher films. Also, the removal of oleate ligands on PbSe requires a higher temperature than for PbS films due to the presence of more ligands. The higher temperature aids in

the removal of oleate ligands because oleate has a boiling point of 260 °C. Preliminary results for PbSe NCs solar cells show efficiencies about tens times lower than the PbS solar cells.

#### 4. Conclusions

In order to make more efficient PV devices that harvest light in the NIR, we reported the fabrication and characterization a solution-processable bilayer hybrid solar cell. This design gave us the opportunity to process the NC layer before the conjugated polymer layer was deposited, unlike previous hybrid bulk heterojunctions solar cells. The NC portion of the active layer was achieved by using ethyl acetate in the NC solution and gently heating the NC film, which partially removed the oleate ligands and cross-linked the NCs. The results indicated that the surface ligands of PbS nanocrystals play an important role in determining the surface roughness and morphology of PbS/P3HT interface, thereby affecting the power conversion efficiency of solar cells. Quantum size effects are anticipated to be a factor in NC solar cell efficiency, however such effects can also be entangled with sample-dependent morphological effects and could not be discerned. Furthermore, Table 1 established that the post-production treatment increased the PV properties owing to polymer crystallization. In summary, each fabrication component was systematically optimized to obtain an effective IV–VI NC/polymer solar cell design.

#### Acknowledgments

The Natural Sciences and Engineering Research Council, Canada and Ontario Graduate Scholarship Program, Canada are gratefully acknowledged for financial support. The authors wish to thank Q. Song for synthesizing the PbSe NCs.

#### References

- [1] S.E. Shaheen, D.S. Ginley, G.E. Jabbour, Organic-based photovoltaics toward low-cost power generation, *MRS Bull.* 30 (2005) 10–19.
- [2] G.D. Scholes, G. Rumbles, Excitons in nanoscale systems, *Nat. Mater.* 5 (2006) 683–696.
- [3] E. Arici, H. Hoppe, F. Schaffler, D. Meissner, M.A. Malik, N.S. Sariciftci, Morphology effects in nanocrystalline CuInSe<sub>2</sub>-conjugated polymer hybrid systems, *Appl. Phys. A* 79 (2004) 59–64.
- [4] S. Gunes, H. Neugebauer, N.S. Sariciftci, H. Roither, M. Kovalenko, G. Pillwein, W. Heiss, Hybrid solar cells using HgTe nanocrystals and nanoporous TiO<sub>2</sub> electrodes, *Adv. Funct. Mater.* 16 (2006) 1095–1099.
- [5] I. Gur, N.A. Fromer, A.P. Alivisatos, Controlled assembly of hybrid bulk-heterojunction solar cells by sequential deposition, *J. Phys. Chem. B* 110 (2006) 25543–25546.
- [6] P. Ravirajan, S.A. Haque, J.R. Durrant, D.D.C. Bradley, J. Nelson, The effect of polymer optoelectronic properties on the performance of multilayer hybrid polymer/TiO<sub>2</sub> solar cells, *Adv. Funct. Mater.* 15 (2005) 609–618.
- [7] H. Hoppe, D.A.M. Egbe, D. Muhlbacher, N.S. Sariciftci, Photovoltaic action of conjugated polymer/fullerene bulk heterojunction solar cells using novel PPE-PPV copolymers, *J. Mater. Chem.* 14 (2004) 3462–3467.
- [8] C. Waldauf, M.C. Scharber, P. Schilinsky, J.A. Hauch, C.J. Brabec, Physics of organic bulk heterojunction devices for photovoltaic applications, *J. Appl. Phys.* 99 (2006).
- [9] A. Watt, E. Thomsen, P. Meredith, H. Rubinsztein-Dunlop, A new approach to the synthesis of conjugated polymer-nanocrystal composites for heterojunction optoelectronics, *Chem. Commun.* (2004) 2334–2335.

- [10] S.E. Shaheen, C.J. Brabec, N.S. Sariciftci, F. Padinger, T. Fromherz, J.C. Hummelen, 2.5% efficient organic plastic solar cells, *Appl. Phys. Lett.* 78 (2001) 841–843.
- [11] B.Q. Sun, H.J. Snaith, A.S. Dhoot, S. Westenhoff, N.C. Greenham, Vertically segregated hybrid blends for photovoltaic devices with improved efficiency, *J. Appl. Phys.* 97 (2005).
- [12] P.A.C. Quist, W.J.E. Beek, M.M. Wienk, R.A.J. Janssen, T.J. Savenije, L.D.A. Siebbeles, Photogeneration and decay of charge carriers in hybrid bulk heterojunctions of ZnO nanoparticles and conjugated polymers, *J. Phys. Chem. B* 110 (2006) 10315–10321.
- [13] W.U. Huynh, J.J. Dittmer, A.P. Alivisatos, Hybrid nanorod-polymer solar cells, *Science* 295 (2002) 2425–2427.
- [14] J. Nelson, *The Physics of Solar Cells*, Imperial College Press, London, 2003.
- [15] C. Winder, N.S. Sariciftci, Low bandgap polymers for photon harvesting in bulk heterojunction solar cells, *J. Mater. Chem.* 14 (2004) 1077–1086.
- [16] A. Dhanabalan, J.K.J. van Duren, P.A. van Hal, J.L.J. van Dongen, R.A.J. Janssen, Synthesis and characterization of a low bandgap conjugated polymer for bulk heterojunction photovoltaic cells, *Adv. Funct. Mater.* 11 (2001) 255–262.
- [17] R.Q. Yang, R.Y. Tian, J.G. Yan, Y. Zhang, J. Yang, Q. Hou, W. Yang, C. Zhang, Y. Cao, Deep-red electroluminescent polymers: synthesis and characterization of new low-band-gap conjugated copolymers for light-emitting diodes and photovoltaic devices, *Macromolecules* 38 (2005) 244–253.
- [18] S.A. McDonald, G. Konstantatos, S.G. Zhang, P.W. Cyr, E.J.D. Klem, L. Levina, E.H. Sargent, Solution-processed PbS quantum dot infrared photodetectors and photovoltaics, *Nat. Mater.* 4 (2005) 138–214.
- [19] D.H. Cui, J. Xu, S.Y. Xu, G. Paradee, B.A. Lewis, M.D. Gerhold, Infrared photodiode based on colloidal PbSe nanocrystal quantum dots, *IEEE Trans. Nanotechnol.* 5 (2006) 362–367.
- [20] A.A.R. Watt, D. Blake, J.H. Warner, E.A. Thomsen, E.L. Tavenner, H. Rubinsztein-Dunlop, P. Meredith, Lead sulfide nanocrystal: conducting polymer solar cells, *J. Phys. D: Appl. Phys.* 38 (2005) 2006–2012.
- [21] A.B. Doust, X.J. Yang, T.E. Dykstra, K. Koo, G.D. Scholes, Light-harvesting antennae for polymer solar cells, *Appl. Phys. Lett.* 89 (2006) 213505.
- [22] Y.X. Liu, M.A. Summers, C. Edder, J.M.J. Frechet, M.D. McGehee, Using resonance energy transfer to improve exciton harvesting in organic–inorganic hybrid photovoltaic cells, *Adv. Mater.* 17 (2005) 2960–2964.
- [23] M.A. Hines, G.D. Scholes, Colloidal PbS nanocrystals with size-tunable near-infrared emission: observation of post-synthesis self-narrowing of the particle size distribution, *Adv. Mater.* 15 (2003) 1844–1849.
- [24] A.J. Nozik, Quantum dot solar cells, *Physica E: Low Dimens. Syst. Nanostruct.* 14 (2002) 115–120.
- [25] R.D. Schaller, V.M. Agranovich, V.I. Klimov, High-efficiency carrier multiplication through direct photogeneration of multi-excitons via virtual single-exciton states, *Nat. Phys.* 1 (2005) 189–194.
- [26] R.D. Schaller, V.I. Klimov, Non-poissonian exciton populations in semiconductor nanocrystals via carrier multiplication, *Phys. Rev. Lett.* 96 (2006) 97402.
- [27] R.J. Ellingson, M.C. Beard, J.C. Johnson, P.R. Yu, O.I. Micic, A.J. Nozik, A. Shabaev, A.L. Efros, Highly efficient multiple exciton generation in colloidal PbSe and PbS quantum dots, *Nano Lett.* 5 (2005) 865–871.
- [28] I. Gur, N.A. Fromer, M.L. Geier, A.P. Alivisatos, Air-stable all-inorganic nanocrystal solar cells processed from solution, *Science* 310 (2005) 462–465.
- [29] S.A. Majetich, A.C. Carter, Surface effects on the optical-properties of cadmium selenide quantum dots, *J. Phys. Chem.* 97 (1993) 8727–8731.
- [30] W.U. Huynh, J.J. Dittmer, W.C. Libby, G.L. Whiting, A.P. Alivisatos, Controlling the morphology of nanocrystal–polymer composites for solar cells, *Adv. Funct. Mater.* 13 (2003) 73–79.
- [31] L. Bakueva, S. Musikhin, M.A. Hines, T.W.F. Chang, M. Tzolov, G.D. Scholes, E.H. Sargent, Size-tunable infrared (1000–1600 nm) electroluminescence from PbS quantum-dot nanocrystals in a semiconducting polymer, *Appl. Phys. Lett.* 82 (2003) 2895–2897.
- [32] T.W.F. Chang, S. Musikhin, L. Bakueva, L. Levina, M.A. Hines, P.W. Cyr, E.H. Sargent, Efficient excitation transfer from polymer to nanocrystals, *Appl. Phys. Lett.* 84 (2004) 4295–4297.
- [33] S. Zhang, P.W. Cyr, S.A. McDonald, G. Konstantatos, E.H. Sargent, Enhanced infrared photovoltaic efficiency in PbS nanocrystal/semiconducting polymer composites: 600-fold increase in maximum power output via control of the ligand barrier, *Appl. Phys. Lett.* 87 (2005) 233101.
- [34] A. Maria, P.W. Cyr, E.J.D. Klem, L. Levina, E.H. Sargent, Solution-processed infrared photovoltaic devices with >10% monochromatic internal quantum efficiency, *Appl. Phys. Lett.* 87 (2005) 213112.
- [35] D.H. Cui, J. Xu, T. Zhu, G. Paradee, S. Ashok, M. Gerhold, Harvest of near infrared light in PbSe nanocrystal–polymer hybrid photovoltaic cells, *Appl. Phys. Lett.* 88 (2006) 183111.
- [36] W.W. Yu, J.C. Falkner, B.S. Shih, V.L. Colvin, Preparation and characterization of monodisperse PbSe semiconductor nanocrystals in a noncoordinating solvent, *Chem. Mater.* 16 (2004) 3318–3322.
- [37] K.K. Rao, D.O. Hall, N. Vlachopoulos, M. Gratzel, M.C.W. Evans, M. Seibert, Photoelectrochemical responses of photosystem-II particles immobilized on dye-derivatized TiO<sub>2</sub> films, *J. Photochem. Photobiol. B* 5 (1990) 379–389.
- [38] G. Yu, J. Gao, J.C. Hummelen, F. Wudl, A.J. Heeger, Polymer photovoltaic cells—enhanced efficiencies via a network of internal donor–acceptor heterojunctions, *Science* 270 (1995) 1789–1791.
- [39] M.C. Hanna, A.J. Nozik, Solar conversion efficiency of photovoltaic and photoelectrolysis cells with carrier multiplication absorbers, *J. Appl. Phys.* 100 (2006) 074510.
- [40] E.A. Weiss, M.R. Wasielewski, M.A. Ratner, Molecular wires: from design to properties, *Top. Curr. Chem.* (2005) 103–133.
- [41] F.C. Grozema, P.T. van Duijnen, Y.A. Berlin, M.A. Ratner, L.D.A. Siebbeles, Intramolecular charge transport along isolated chains of conjugated polymers: effect of torsional disorder and polymerization defects, *J. Phys. Chem. B* 106 (2002) 7791–7795.
- [42] S. Günes, K.P. Fritz, H. Neugebauer, N.S. Sariciftci, S. Kumar, G.D. Scholes, Hybrid solar cells using PbS nanoparticles, *Solar Energy Mater. Solar Cells* 91 (2007) 420–423.
- [43] C.B. Murray, C.R. Kagan, M.G. Bawendi, Synthesis and characterization of monodisperse nanocrystals and close-packed nanocrystal assemblies, *Annu. Rev. Mater. Sci.* 30 (2000) 545–610.
- [44] C.B. Murray, S.H. Sun, W. Gaschler, H. Doyle, T.A. Betley, C.R. Kagan, Colloidal synthesis of nanocrystals and nanocrystal superlattices, *IBM J. Res. Dev.* 45 (2001) 47–56.
- [45] P. Guyot-Sionnest, C. Wang, Fast voltammetric and electrochromic response of semiconductor nanocrystal thin films, *J. Phys. Chem. B* 107 (2003) 7355–7359.
- [46] G. Konstantatos, I. Howard, A. Fischer, S. Hoogland, J. Clifford, E. Klem, L. Levina, E.H. Sargent, Ultrasensitive solution-cast quantum dot photodetectors, *Nature* 442 (2006) 180–183.
- [47] Y. Zhao, G.X. Yuan, P. Roche, M. Leclerc, A calorimetric study of the phase-transitions in poly(3-hexylthiophene), *Polymer* 36 (1995) 2211–2214.
- [48] J.J. Dittmer, E.A. Marseglia, R.H. Friend, Electron trapping in dye/polymer blend photovoltaic cells, *Adv. Mater.* 12 (2000) 1270–1274.
- [49] F. Padinger, R.S. Rittberger, N.S. Sariciftci, Effects of post-production treatment on plastic solar cells, *Adv. Funct. Mater.* 13 (2003) 85–88.
- [50] A.J. Mozer, N.S. Sariciftci, A. Pivrikas, R. Osterbacka, G. Juska, L. Brassat, H. Bassler, Charge carrier mobility in regioregular poly(3-hexylthiophene) probed by transient conductivity techniques: a comparative study, *Phys. Rev. B* 71 (2005) 035214.

- [51] W.J. Mitchell, P.L. Burn, R.K. Thomas, G. Fragneto, Probing the polymer-electrode interface using neutron reflection, *Appl. Phys. Lett.* 82 (2003) 2724–2726.
- [52] W.J. Mitchell, P.L. Burn, R.K. Thomas, G. Fragneto, J.P.J. Markham, I.D.W. Samuel, Relating the physical structure and optical properties of conjugated polymers using neutron reflectivity in combination with photoluminescence spectroscopy, *J. Appl. Phys.* 95 (2004) 2391–2396.
- [53] W.U. Huynh, X.G. Peng, A.P. Alivisatos, CdSe nanocrystal rods/poly(3-hexylthiophene) composite photovoltaic devices, *Adv. Mater.* 11 (1999) 923–927.
- [54] J. Xu, D.H. Cui, T. Zhu, G. Paradee, Z.Q. Liang, Q. Wang, S.Y. Xu, A.Y. Wang, Synthesis and surface modification of PbSe/PbS core-shell nanocrystals for potential device applications, *Nanotechnology* 17 (2006) 5428–5434.